MODIFICATION OF A SPARE SEPTUM MAGNET FOR SNS RING INJECTION DUMP BEAM LINE *

J. G. Wang #
SNS/ORNL, Oak Ridge, TN 37831-6476, U.S.A.

Abstract

The SNS ring injection dump septum magnet suffered severe beam losses in commissioning and early operations. These beam losses were caused by a number of design and operation problems including inadequate aperture of the injection dump septum. After taking a few mitigating actions, we modified a spare septum to improve its performance for further reducing particle losses in the device. This paper reports the detailed modification results, including 3D particle tracking and experimental measurements.

INTRODUCTION

The Spallation Neutron Source (SNS) ring injection [1, 2] is partially depicted in a 3D model as shown in Fig. 1. An H^- beam from the SNS linac strikes a primary foil (F1), after which majority of the particles is fully striped off two electrons and becomes the proton particles. These protons go through chicane dipoles D3 and D4, and get into the ring as a circulating beam. A small portion of the incoming H^- beam is only partially stripped and becomes H^0 particles. These H^0 particles drift forward and strike a secondary foil (F2), after which they all become the protons. These H^0-protons are bent by D4 first and then transported through an Injection Dump Septum Magnet (IDSM) to an injection dump further downstream. There is even a smaller portion of the incoming H^- beam, which misses F1 and is bent by D2 fringe field and D3 until it strikes F2 and becomes the protons. These H^--protons are bent also by D4 first and then transported through IDSM to the dump. Both the H^0-protons and H^--protons are so called waste beams.

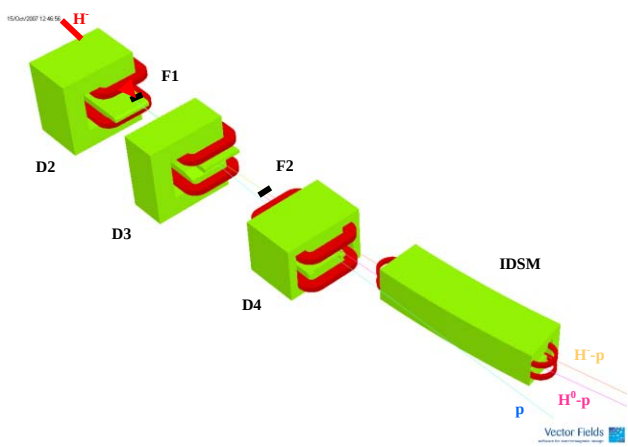

Figure 1: A 3D simulation model for SNS ring injection dump beam line.

*Work supported by US DOE contract No. DE-AC05-00OR22725.
#jgwang@ornl.gov

In SNS commissioning and early operations, particle losses in IDSM were the heaviest in the machine. 3D simulation studies showed a clear picture of the particle loss mechanisms [3, 4]. Many H^--protons had excessive vertical motion and hit the upper surface of the IDSM vacuum chamber. This was due to incorrect D4 position, which was mitigated later. The H^0-protons inside IDSM were too close to the right edge of its chamber; many of them were lost horizontally in the septum. This was caused by incorrect chicane dipole settings, and much effort was made to remedy them. In addition, the IDSM aperture was inadequate in both the vertical and horizontal directions that made it difficult to transport the waste beams through. Thus, we modified a spare IDSM.

MODIFICATION

A modified IDSM is shown in a 3D model in Fig. 2 [5]. The main purpose is to enlarge its aperture as much as possible. First, the vertical gap is increased by 2 cm that provides both the H^--proton and H^0-proton particles more clearance in the y-direction. Second, good field region for the H^0-protons is further extended from the pole-tip edge toward the septum plate, where it happens that there is some space available. Thus, the vacuum chamber can be accordingly enlarged by almost 3 cm, which gives the H^0-proton particles significantly more clearance in the x-direction. Third, we add specially designed z-bumps at the entrance face that further push the H^0-protons inward in IDSM. Fourth, the septum plate has to be extended out in order to shield the adjacent proton beam pipe from magnetic fringe field of IDSM.

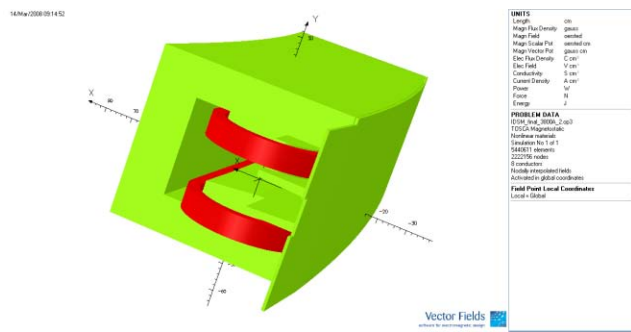

Figure 2. Modified septum model (entrance view).

Figure 3 shows the IDSM vacuum chamber aperture before and after the modification. Both the waste beams gain more clearance in the vertical direction with the H^--protons benefited more since they pass through the left side of the chamber. The H^0-proton beam gains exclusively 2.95 cm more clearance in the horizontal direction that reduces their losses inside IDSM.

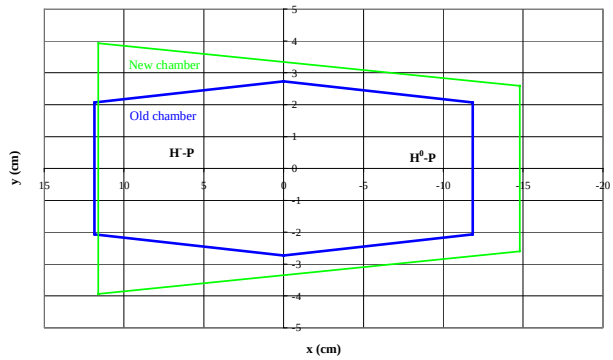

Figure 3. IDSM vacuum chamber inner surface dimension before and after modification.

SIMULATION

3D simulation models are built with OPERA-3d/TOSCA [6] to study field distributions and particle trajectories in IDSM. Figure 4 shows the magnetic bending field B_y across the gap on the mid-plane. The blue curve is for the old septum which operated at 2914 A. The red curve is from the modified magnet, which would operate at 3800 A. Though the field strength on the right side (for the H^0-protons) is smaller in the modified septum, the integrated field is about the same since new z-bumps are added on this side. The main disadvantage of enlarging the vertical gap is the rather lower gradient for the H^0-proton particles. The two black and two red vertical lines indicate the positions of the old and new vacuum chamber inner surfaces.

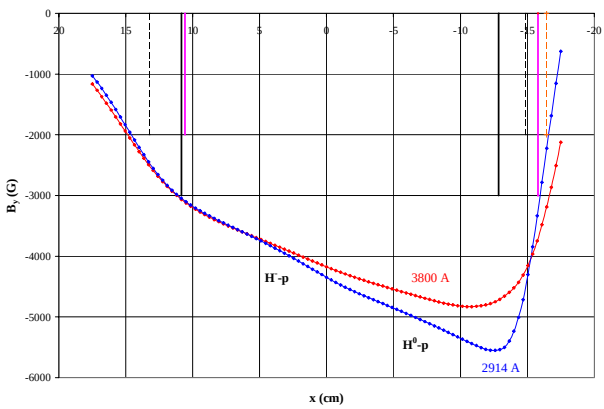

Figure 4. Magnetic field B_y across IDSM gap.

The field B_y along two selected particle trajectories is plotted in Fig. 5. For the H^--protons, the field B_y versus z is very close before and after the modification. The integrated field in the old septum is -0.790 T-m, which yields a bending angle of 8.00° at 1 GeV; while it is -0.786 T-m, or 7.96°, in the modified one. For the H^0-proton trajectory, the difference in field distribution between the old and new septum is quite obvious. But, the integrated field is still fairly close in the two cases. The integrated field in the old septum is -1.034 T-m, corresponding to a bending angle of 10.5°, while it is -1.004 T-m or 10.2° in the new one. More importantly, the integrated field before the magnet entrance face in the modified septum is significantly larger than that in the old one due to the new z-bumps, which steer the H^0-protons slightly inwards. This is good in reducing the H^0-proton losses in the x-direction around the middle of the magnet. In the modified septum the average field $\langle B_y \rangle$ from z=50 to 150 cm is -4680 G for the H^0-proton trajectory. This yields a hard edge length of 2.15 m. For the H^--proton trajectory, the average field $\langle B_y \rangle$ from z=50 to 150 cm is -3797 G, leading to a hard edge length of 2.07 m.

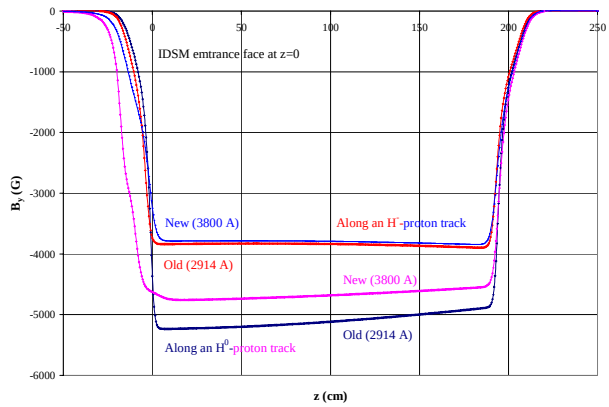

Figure 5. Bending field B_y vs. z along particle trajectories.

Figure 6 shows the two waste beam centroids in the x-z plane. The initial conditions in the front of the septum are determined from the production chicane setting after D4 is moved. The H^--proton centroid trajectory in the modified model is almost the same as before, so the two trajectories overlap. The H^0-protons are pushed slightly inward by the new z-bumps. It is about 0.6 cm closer to the axis at z=100 cm where the particles were lost most. The new z-bumps form a small steering dipole, which has an integrated bending field of about 0.04 T-m, yielding a bending angle of about 7 mrad at 1 GeV. The new vacuum chamber inner surface is depicted by the green, dashed curve, which is 2.95 cm away from the original one. This new boundary should provide good space for the H^0-protons and reduces their losses in the magnet.

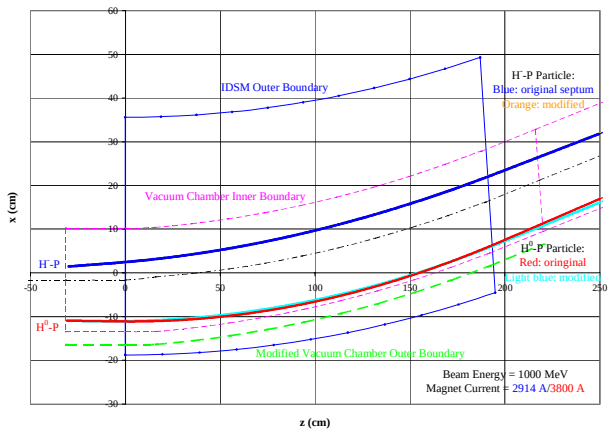

Figure 6. Waste beam trajectories in the septum before and after modification.

MEASUREMENT

The integrated bending field of the modified septum is measured by a flip coil and is compared with 3D simulation results. An experimental setup with the septum exit view is shown in Fig. 7. The flip coil is a BNL product with the dimensions of 365.76x1.27x1.27 cm^3. The coil has 20 turns of conducting wires in a single layer with a width of 1.2974 cm [7]. An aluminum plate is made in house to position the coil. There are four tracks on the plate, two each for H^0-proton and H^--proton particle trajectories. Each track follows the natural curvature inside the septum and is perpendicular to the magnet faces outside. The four track positions from the septum axis are 10.49782, 5.41782, -3.72618, and -9.56818 cm, respectively. Each track is determined by five position pins, against which the coil is positioned before and after a flip. The plate is located in the septum in such a way that the coil winding is on the mid-plane.

Figure 7. Measurement of modified septum by a flip coil.

The measured Integrated Transfer Function (ITF) for 1 GeV operation range is shown in Fig. 8. The H^0-proton trajectories go through the region between tracks 1 and 2. Its integrated field at 3800 A is about 1 T-m. The H^--proton particle trajectories go through the region between tracks 3 and 4, with a maximum integrated field close to 0.8 T-m at 3800 A. In the plot we also show the 3D simulation data at 3800 A, indicated by larger diamonds. The difference between the measurement and simulation is less than 1%. The agreement is pretty good. Figure 9 shows the integrated gradient in the two waste beam regions. It is about 1 T for the H^0-proton particles and more than 2 T for the H^--proton particles. These numbers are consistent with the central gradients shown in Fig. 4, considering that the hard edge length of the modified septum is a little more than 2 m. The difference in the integrated gradient between the measurements and simulations is also marked in the figure. The lower gradient for the H^0-proton particles is a result of the increased gap. This is disadvantageous for operation. Similar measurements are also performed for the 1.3 GeV operation range. The measurement data show satisfactory performance of the modified septum. The fringe field on the proton beam line is measured by a Hall probe. Though the extended septum plate reduces the effect of magnetic fringe field on the circulating proton beam, further shielding of the proton beam pipe by μ-metal is still required.

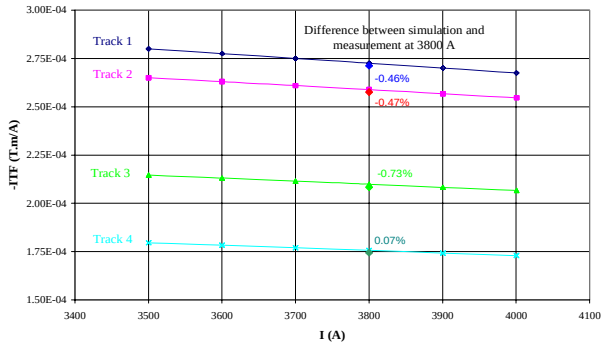

Figure 8. ITF of modified septum for 1 GeV operation.

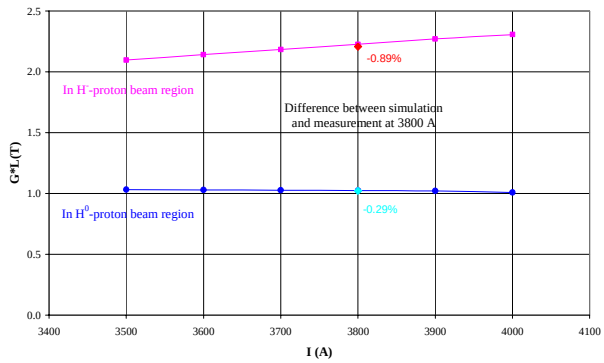

Figure 9. Integrated gradient of modified IDSM for 1 GeV operation.

ACKNOLEDGEMENTS

The author would like to thank G. Murdoch, D. Lousteau, J. Galambos, M. Plum, T. Hunter, D. LeBon, S. Heimsoth, M. Holding, R. Savino, J. Error, P. Wanderer, A. Jain, J. Jackson, and J. Cintorino for their help and support in this work.

REFERENCES

[1] J. Wei, J. Beebe-Wang, M. Blaskiewicz, J. Brodowski, A. Fedotov, C. Gardner, Y.Y. Lee, D. Raparia, V. Danilov, J. Holmes, C. Prior, G. Rees, S. Machida, in Proc. of PAC01, Chicago, IL, p.2560.

[2] D. Raparia for the SNS collaboration, in Proc. of PAC05, Knoxville, TN, p.553.

[3] J. G. Wang, in Proc. of PAC07, Albuquerque, NM, p.3660.

[4] J. G. Wang and M.A. Plum, Phys. Rev. ST Accel. Beams **11**, 014002 (2008). http://prstab.aps.org/abstract/PRSTAB/v11/i12/e014012

[5] J. G. Wang, SNS-NOTE-MAG-181, March 28, 2008.

[6] Vector Fields, software for electromagnetic design, http://www.vectorfields.com/

[7] J. Jackson, private communication.